Localized itinerant electrons and unique magnetic properties of $SrRu_2O_6$

S. Streltsov,[1,2] I. I. Mazin,[3] and K. Foyevtsova[4]

[1]*M.N. Miheev Institute of Metal Physics of Ural Branch of Russian Academy of Sciences, 620137, Ekaterinburg, Russia*

[2]*Theoretical Physics and Applied Mathematics Department, Ural Federal University, Mira St. 19, 620002 Ekaterinburg, Russia*

[3]*Code 6393, Naval Research Laboratory, Washington, DC 20375, USA*

[4]*Quantum Matter Institute, University of British Columbia, Vancouver, British Columbia, Canada V6T 1Z4*

(Received 11 August 2015; published 12 October 2015)

$SrRu_2O_6$ has unique magnetic properties. It is characterized by a very high Néel temperature, despite its quasi-two-dimensional structure, and has a magnetic moment more than twice reduced compared to the formal ionic count. First-principles calculations show that only an ideal Néel ordering in the Ru plane is possible, with no other metastable magnetic solutions, and, highly unusually, yield dielectric gaps for both antiferromagnetic and nonmagnetic states. We demonstrate that this strange behavior is the result of the formation of very specific electronic objects, recently suggested for a geometrically similar Na_2IrO_3 compound, whereby each electron is well localized on a particular Ru_6 hexagon, and completely delocalized over the corresponding six Ru sites, thus making the compound *both* strongly localized and highly itinerant.

DOI: 10.1103/PhysRevB.92.134408 PACS number(s): 75.50.Ee, 71.15.Mb, 75.30.Et, 71.27.+a

The recently discovered [1] $SrRu_2O_6$ has attracted considerable attention because, despite being a very two-dimensional (2D) material, it shows an exceptionally high Néel temperature of ∼560 K [2,3]. As we will argue in this paper, this is by far not the only, and maybe not even the most intriguing, property of this material. Ru^{5+} has a half-filled t_{2g} electronic shell, and exhibits insulating behavior. Naturally, it was interpreted as a Slater insulator (maybe Mott-enhanced), with Ru in the high spin state $S = 3/2$. However, the experimentally measured ordered magnetic moment is only $M = 1.3$–$1.4\mu_B$ [2,3], 2.3 times smaller than expected for $S = 3/2$ ($M = 3\mu_B$). This was ascribed to hybridization with oxygen [2–4], but it should be noted that such strong suppression of magnetic moment in a good insulator is unheard of. Even in the metallic $SrRuO_3$ the hybridization suppresses the total magnetic moment of Ru^{4+} only from 2 to $1.7\mu_B$, and in Sr_2YRuO_6 Ru^{5+} has essentially exactly $3\mu_B$, with basically the same Ru-O distances as in $SrRu_2O_6$ [5]. Hiley *et al.* [2] mention the case of Li_3RuO_4 [6], where a suppression down to $M = 2.0\mu_B$ was reported for the same oxidation state, which is, however, still twice smaller a reduction compared to $SrRu_2O_6$, and the material might actually be a metal (no transport data have been published).

Electronic structure calculations [3,4] so far have not resolved the mystery, but have only added to the confusion. It was found that only the ideal Néel state can be stabilized in the calculations, even though ions with $S = 3/2$ are usually very stable, and while they disorder with temperature, never lose their magnetic moment completely. At the same time the moment found in the calculations matches the experimentally measured one within 8%, suggesting that the role of Coulomb correlations beyond the standard density functional theory (DFT) is negligible [7]. The instability of the ferromagnetic (FM) state was traced down to the presence of a dielectric gap in nonmagnetic calculations [4], but that essentially translates one mystery into another: why does a highly symmetric Ru sublattice, with no dimerization or clusterization, with a half-filled t_{2g} band, show a sizable nonmagnetic gap? Singh mentions [4] that the gap is allowed by symmetry, since the unit cell includes two Ru atoms that can, in principle, form a bonding and an antibonding bands, but does not elaborate about how a structure with each Ru having three equivalent bonds manages to develop a bonding-antibonding splitting.

Similarly, it was pointed out that, even though $SrRu_2O_6$ is extremely 2D magnetically, there is still some residual interlayer coupling, $J_\perp M^2 \approx 1.5$ meV, as well as a single-ion magnetic anisotropy, estimated to be ≈1.4 meV/Ru [4]. It was suggested that the anisotropy [4] or interlayer coupling [3] are responsible for the large T_N, implying that the (unknown) mean field transition temperature is extremely high. Tian *et al.* [3] attempted to describe this system by a three nearest-neighbor Heisenberg model with parameters derived within the perturbation theory in the limit of a Hubbard U much larger than the hopping, $U \gg t$. However, the fact that ferromagnetic arrangement is completely unstable (in fact, as we show below, no parallel nearest-neighbor moments are stable), indicates that the system is strongly non-Heisenberg, casting very strong doubt on the relevance of such models. Additionally, the fact that the system is very weakly correlated makes such a perturbation theory unphysical. Similarly, Hiley *et al.* [2] used a hybrid functional that overestimates the equilibrium magnetic moment and thus the exchange parameters [8], as well as yields a very large band gap of 2.15 eV, totally inconsistent with the observed weak temperature dependence of the resistivity.

An explanation of all these oddities can be consistently found in the so-called molecular orbitals (MO) picture, which was first brought up in connection to Na_2IrO_3 [9] and later found also in $RuCl_3$ [10]. Basically, this picture is based on the idea that for ideal 90° Ru-O-Ru bond angles (the actual angles are 101°) the O-assisted Ru-Ru hopping is only allowed for one particular pair of the t_{2g} orbitals for each hexagonal bond, denoted t_1' in Ref. [9]. If all other hoppings are neglected, it leads to a curious situation where every electronic state is fully delocalized over a particular hexagon, but never leaves this hexagon. One can say that the electrons are fully localized (form nondispersive levels) and fully delocalized (each state is an equal weight combination of six orbitals belonging to six different sites). If a direct overlap of the t_{2g} orbitals (which

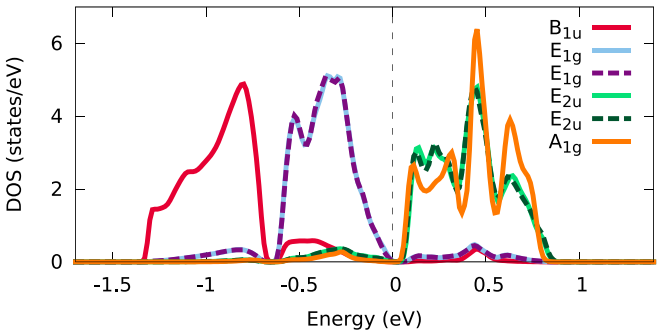

FIG. 1. (Color online) Density of states (DOS) projected on molecular orbitals of different symmetries in nonmagnetic GGA calculations (WIEN2k results). The Fermi energy is set to zero.

always exists in the common edge geometry) is included, as well as deviations of the angle from 90°, two more hoppings emerge: one between the same orbitals on the neighboring sites t_1, and the other an O-assisted second neighbor hopping between unlike orbitals t_2'. As long as t_1' is dominant, the MO model still applies, and can be readily solved. The solution entails six bands, A_{1g}, E_{2u}, E_{1g}, and B_{1u} (the E bands being double degenerate in each spin channel), whose dispersion is controlled by t_1, and whose centers are located at $2(t_1'+t_2')$, $(t_1'-t_2')$, $-(t_1'+t_2')$, and $-2(t_1'-t_2')$, respectively. In Na_2IrO_3 $t_1' \approx -3t_2'$, so that the A_{1g} and E_{2u} practically merge. This accidental degeneracy also leads to much stronger spin-orbit effects than would have been possible had the MO bands remained well separated, and to considerable destruction of the MO picture in the relativistic case. On the other hand, the hopping parameters for $SrRu_2O_6$, as calculated in Ref. [11], are similar to those in Na_2IrO_3, in the sense that again $t_1' = 300$ meV is by far the largest hopping, and the only other sizable hoppings are $t_1 = 160$ meV and $-t_2' \approx 100$–110 meV. Note that here $|t_2'|$ is again about $1/3$ of t_1'. Thus, the A_{1g} and E_{2u} bands merge, while E_{1g} and B_{1u} remain separated, as one can see in Fig. 1. Projecting the density of states onto MOs, we observe that the predicted characters are very well reproduced. The distance between the centers of the E_{2u} and E_{1g} bands is about 0.8 eV, and their width is about 0.6–0.7 eV, thus providing for a small gap of ≈50 meV.

It is instructive to compare $SrRu_2O_6$ with Na_2IrO_3 and with Li_2RuO_3. All these compounds share the same crystallographic motif, but feature a different number of d electrons: 5, 4, or 3. In the iridate, a single hole in the upper A_{1g} singlet is prone to both strong correlations and, due to near degeneracy between A_{1g} and E_{2u}, to spin-orbit interaction. As a result, as one increases the spin-orbit coupling, the A_{1g} singlet is gradually transformed into the $j_{\rm eff} = 1/2$ singlet [9]. Either way, a half-filled singlet triggers Mott physics even if the Hubbard U is small. This transformation controls most of the interesting physics in this compound. Li_2RuO_3 has two d holes, providing it with an opportunity to form strongly bound covalent dimers. This is exactly what happens, and the MO on the hexagons transforms to an MO on the Ru dimers resulting in the spin singlet ground state [12]. Neither Mott nor spin-orbit physics is relevant on the background of the strong covalent bonding in dimers. Finally, $SrRu_2O_6$ has the six MO bands half-filled, and the gap is formed between the lower and the upper MO triads. Similar to Li_2RuO_3, both Mott and spin-orbit effects are of minor importance, and the gap structure inherent to the MO picture gives rise to unique magnetic properties.

Let us now turn to the energetics of the material. First, we have confirmed, using the WIEN2k package [13,14], the numbers published by Singh [4] regarding the interplanar coupling, single-site anisotropy, and Ru magnetic moment. We also confirmed that the ferromagnetic structure cannot be stabilized. Moreover, the so-called stripy and zigzag magnetic patterns [9], where one or two out of three bonds are ferromagnetic, and the net moment is zero, cannot be stabilized. This indicates that besides the obvious influence of the nonmagnetic gap there are other factors strongly disfavoring ferromagnetic bonds. In fact, given that the gap value is ten times smaller than Ru Stoner factor [5], and the calculated magnetic moment in the Néel state is $\sim 1.3\,\mu_B$, it is surprising that the ferromagnetic bonds do not stabilize with a finite moment.

In order to gain more insight into the problem, we turned to the VASP code [14,15], which is faster and has the capability to restrict magnetic moments to a certain direction, or to both a direction and a magnitude (we confirmed that the energies of collinear magnetic states agree with those found in WIEN2k). First, we computed the total energy for a canted antiferromagnet (AFM), restricting the angle with the z axis to be $\pm\phi$ for the two Ru's in the cell. The results are shown in Fig. 2. Note that for the largest canting angle we were able to converge, 35°, the energy of the magnetic state is already higher than that of the nonmagnetic one. Also note how soft the magnetic moments are: despite the sizable equilibrium moment, the energy cost of total suppression of magnetism is less than 80 meV, only 50% larger than the transition temperature. This is, again, an indication of the great role of itinerancy, and specifically, delocalization over Ru_6 hexagons.

Interestingly, suppression of magnetism with canting cannot be described by a naive combination of a local Hamiltonian for itinerant magnets [16], $E = \sum_{i\geqslant 0} a_i M^{2i}$, where M is the magnetization, with a Heisenberg term. While the total energies at a fixed canting angle $\phi \lesssim 35°$ can be very well described by this Hamiltonian with just three terms,

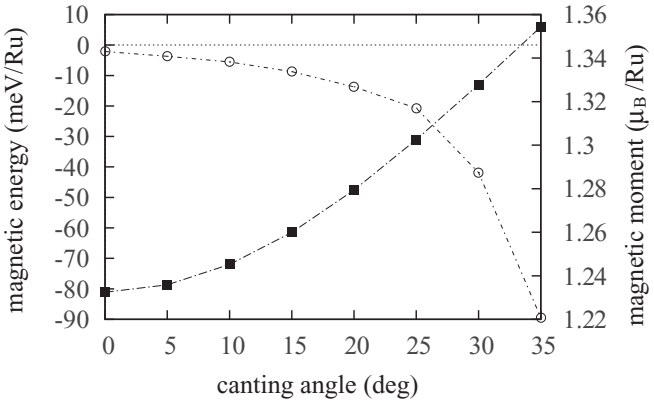

FIG. 2. Magnetic energy (squares) and magnetic moments (circles) as a function of the canting angle of spins, starting from the Néel antiferromagnetic structure. Results are from VASP calculations.

$E(M) - E(0) = a_1 M^2 + a_2 M^4 + a_3 M^6$, not only does the first coefficient show appreciable angular dependence (as in the Heisenberg model), but also the second, and, to a lesser degree, the third. Instead, a good fit could be obtained with the following formula:

$$E = -81.3M^2 + 16.9M^4 + 2.0M^6 + 359.2M^2 \sin^2(\phi) - 165.8M^4 \sin^2(\phi) + 27.6M^6 \sin^2(\phi), \quad (1)$$

in meV/Ru. Note that the angle between the moments is $\theta = \pi - 2\phi$, and that there are 1.5 times more bonds than sites. Thus, the proposed Hamiltonian looks as follows:

$$H = \sum_{\text{sites}} \{98.3M^2 - 66.0M^4 + 15.8M^6\} + \sum_{\substack{\text{n.n.}\\ \text{bonds}}} \{179.6(\mathbf{M}\cdot\mathbf{M}') - 82.9|\mathbf{M}||\mathbf{M}'|(\mathbf{M}\cdot\mathbf{M}') + 13.8|\mathbf{M}|^2|\mathbf{M}'|^2(\mathbf{M}\cdot\mathbf{M}')\}. \quad (2)$$

The Heisenberg term is extremely strong [$JM^2 = \partial H/\partial \cos(\theta) \approx 1600$ K], and, without it, local magnetic moments fail to form.

To this Hamiltonian one needs to add a small interlayer term $\sum J_\perp \mathbf{M}_i \cdot \mathbf{M}_{i'}$, where i and i' belong to the neighboring planes, and the magnetic anisotropy $\sum D M_z^2$, where $J_\perp \approx 0.9$ meV, and $D \approx 0.8$ meV.

In principle, at this point one would need to perform a Monte Carlo simulation using this Hamiltonian and determine the transition temperature. However, it is notoriously difficult to distinguish a Kosterlitz-Thouless phase in a quasi-2D system from the true long range order, so that one should be very skeptical of any Monte Carlo simulation that claims to establish a Néel temperature T_N without first showing that in the isotropic 2D limit T_N truly vanishes. The softness of the moment, expressed via Eq. (2), additionally complicates the simulation. We leave this daunting task to more experienced Monte Carlo simulators, but mention that the numbers that we have deduced are in the right ballpark. For instance, Costa and Pires showed [17] that for the square lattice $T_N/T_{\text{MF}} \approx 0.8(D/J)^{0.2}$. For three neighbors, the mean field transition temperature $T_{\text{MF}} \approx JM^2 \approx 1600$ K, which together with $DM^2 \approx 1.4$ meV results in $T_N \sim 500$ K. On the other hand, for the cubic quasi-2D model with $J_\perp \neq 0$, $D = 0$, Yasuda *et al.* [18] found that $T_N \approx 4.27 JM^2/[3.12 + \log(J/J_\perp)]$, which for our parameters translates into 900 K. Thus, we conclude that (a) the Mermin-Wagner theorem is mainly lifted via the interplanar coupling [3], and not via the single site anisotropy [4], and (b) the softness of the magnetic moment, i.e., longitudinal fluctuations, plays an important role, suppressing T_N by up to a factor of 2.

Let us now discuss how and why MOs support a Néel antiferromagnetism in $SrRu_2O_6$. In the nonmagnetic state, the three lower MO bands, B_{1u} and E_{1g}, are fully occupied. Imposing uniform spin polarization does not change the occupancy of these states, unless the induced exchange splitting is larger than the gap, and this is why the ferromagnetic order is unstable. On the contrary, imposing the staggered magnetic field of $\pm\Delta$ does not break the MO band structure, but rather increases the gap between E_{1g} and E_{2u} (in the lowest order in Δ, by Δ^2/t_1'). In the same order we can calculate the change of the occupancies and find that the spin-up sites acquire magnetization of $5\Delta/2t_1'\,\mu_B$, and the spin-down sites $-5\Delta/2t_1'\,\mu_B$. The signs are consistent with the assumed signs of Δ, which tells us that with sufficiently large Hund's rule coupling the system will become unstable against such a staggered magnetization (but will resist any ferromagnetic component); of course, quantitative analysis is impossible on this level of simplification. Obviously, the equilibrium moment can be anything between 0 and $3\mu_B$. It is not "suppressed" from the putative $S = 3/2$ state, but is set by the interplay between the Hund's rule coupling on Ru and the details of the density of states of MOs. A corollary from the above arguments is that the dielectric gap depends quadratically on the Ru moment; Fig. 3 illustrates that this is indeed the case, to a reasonable accuracy.

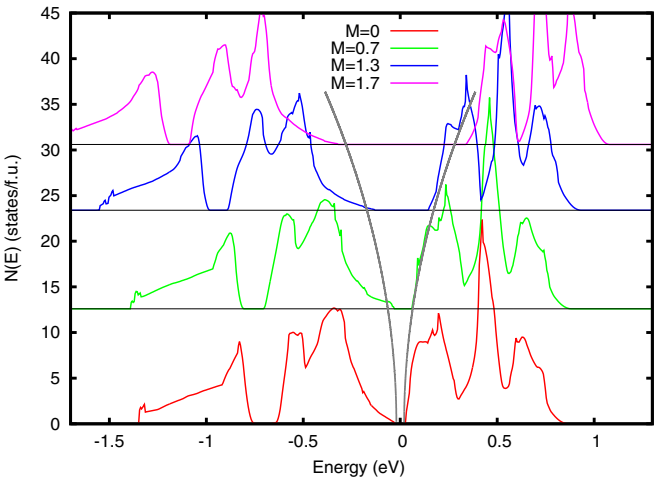

FIG. 3. (Color online) Total density of states (DOS) calculated for several values of Ru moments M in the fixed-spin-moment procedure for the Néel AFM. The black lines illustrate the fact that the band gap is approximately quadratic in M. Results of the VASP calculations.

Let us emphasize that the molecular orbitals are not just another way to describe the electronic structure of $SrRu_2O_6$, but have profound physical meaning. It is instructive to compare it with another recently investigated high-T_N material, $SrTcO_3$, where the transition metal also has a $4d^3$ configuration and $S = 3/2$. It was argued [19] that T_N is so high because $SrTcO_3$ is in an intermediate regime between itinerancy and localization, which is optimal for magnetic interactions. Indeed, LDA + DMFT calculations, well suited to this regime, have been performed by Mravlje *et al.* [19], who found $T_N \approx 2200$ K. The experimental number is about 1100 K. To compare this result with $SrRu_2O_6$, we have also performed LDA + DMFT calculations with the AMULET code [20], using an effective Hamiltonian constructed for Ru t_{2g} orbitals and interaction parameters $U = 2.7$ and $J = 0.3$ eV as calculated in Ref. [3] (parameters for Tc are very similar). The corresponding temperature dependence of the magnetic moment is shown in Fig. 4. Not surprisingly, we found about the same Néel temperature (2000 K) as Mravlje *et al.* [19], and an even larger magnetic moment ($M \approx 2.7$ vs $2.5\mu_B$). The difference, however, is that experimentally in $SrRu_2O_6$ both T_N *and* M are about twice smaller than in

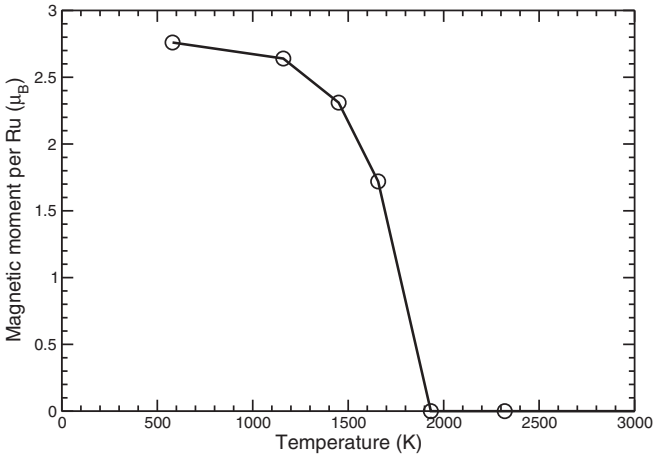

FIG. 4. Magnetic moment as calculated in the LDA + DMFT approach. The continues-time quantum Monte Carlo (CT-QMC) solver [22] was used in these calculations.

$SrTcO_3$. Mravlje *et al.* ascribed their overestimation of T_N to nonlocal fluctuations, missing in the DMFT, but observed no reduction in the ordered moment at all, while in our case the reduction in *both* T_N *and* M^2 is of the same order, about a factor of 4. This clearly indicates that there is a fundamental difference between the two compounds, going much beyond just the difference in dimensionality, which is related to the presence of MOs in one and their absence in the other compound. A proper account of the molecular orbitals within DMFT can only be done in the cluster extension of this method [21], which could shed more light on this compound.

Another interesting question that arises in connection with this material is what would happen if it were doped with, for instance, a rare earth element. To address this scenario, we simulated doping by adding electrons to the system (with a compensating constant background). The energy difference between the FM and Néel AFM states decreases upon electron doping, as seen from Fig. 5. The FM configuration immediately becomes metastable, whereby all doped electrons go into one spin subband, rendering the material is half-metallic. The ground state remains antiferromagnetic, but its energy advantage is gradually decreasing. Thus, one expects that the critical angle ϕ (which was $\sim 35^\circ$ in undoped case) will grow with doping, and the Hamiltonian (2) will be correspondingly modified; this may result in a rapid change of magnetic properties with doping, which deserves further theoretical and experimental investigation.

To summarize, we have found that:

(i) The electronic structure of $SrRu_2O_6$ is dominated by molecular orbitals. Each electron is, to a good approximation, localized on a particular Ru_6 hexagon, and completely delocalized over the corresponding six Ru sites.

(ii) This structure sports an excitation gap that prevents formation of ferromagnetic bonds, but is consistent with nearest-neighbor antiferromagnetism. The corresponding magnetic interactions cannot be mapped onto a localized spin model, be it Heisenberg or biquadratic Hamiltonian with arbitrary long range. Neither can it be described as purely itinerant magnetism, but features interesting elements of both. This

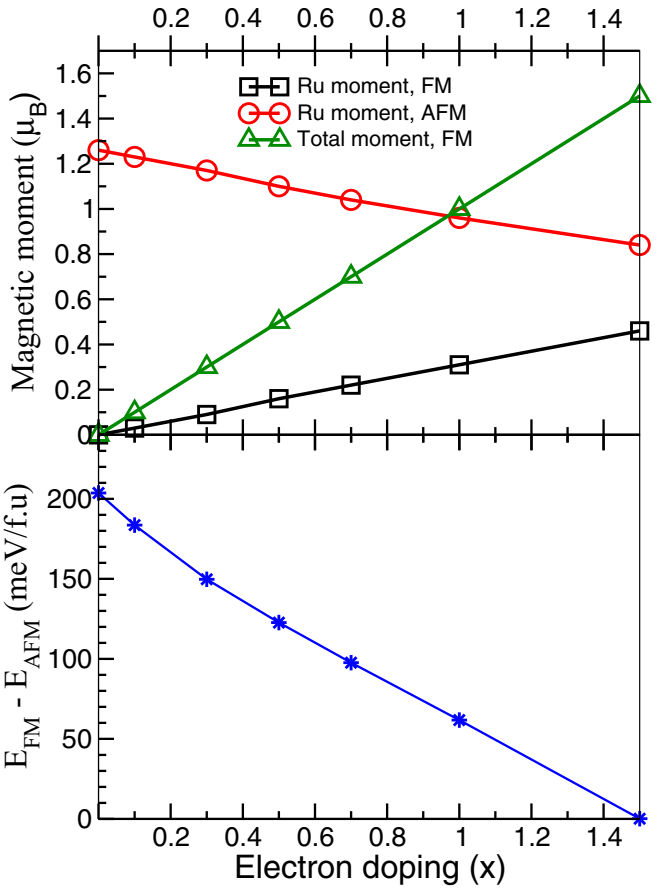

FIG. 5. (Color online) Electron doping dependence of magnetic moments (per Ru and total) and total energy difference between FM and Néel AFM states on the electron doping.

duality reflects the dual character of the electronic structure, where electrons are simultaneously completely delocalized and strongly localized on the Ru hexagons. A corollary is that any deviation from the collinear Néel order is severely punished by kinetic energy, which, in turn, provides for the anomalously large transition temperature.

(iii) The gaps in the nonmagnetic and antiferromagnetic states have the same nature, and one is continuously transformed into the other as the magnetization increases. On the contrary, the ionic picture assigning the moment of $3\mu_B$ to each Ru and associating the gap in magnetic states with spin-up/spin-down splitting is qualitatively incorrect. The observed and calculated magnetic moment of $1.3\mu_B$ is a manifestation of the molecular orbital nature of electronic states, and should not be viewed as a spin $S = 3/2$ reduced by hybridization.

(iv) The magnetic properties of doped $SrRu_2O_6$ (e.g., by Na or La) are expected to be very different from the stoichiometric case. One may anticipate interesting and very different physics emerging, which can be a subject of forthcoming research.

S.S. and I.M. are grateful to R. Valenti and University of Frankfurt (where this work was started) for the hospitality and to A. Ruban, S. Khmelevskii, A. Poteryaev, D. Khomskii, and K. Belashchenko for useful discussions. This work was supported by Civil Research and Development Foundation

via program FSCX-14-61025-0, the Russian Foundation of Basic Research via Grant No. 13-02-00374, Ural branch of Russian academy of Science via program 15-8-2-4 and FASO (theme Electron No. 01201463326). I.M. is supported by ONR through the NRL basic research program.

[1] C. I. Hiley, M. R. Lees, J. M. Fisher, D. Thompsett, S. Agrestini, R. I. Smith, and R. I. Walton, Angew. Chem. Int. Ed. **53**, 4423 (2014).

[2] C. I. Hiley, D. O. Scanlon, A. A. Sokol, S. M. Woodley, A. M. Ganose, S. Sangiao, J. M. De Teresa, P. Manuel, D. D. Khalyavin, M. Walker, M. R. Lees, and R. I. Walton, Phys. Rev. B **92**, 104413 (2015).

[3] W. Tian, C. Svoboda, M. Ochi, M. Matsuda, H. B. Cao, J.-G. Cheng, B. C. Sales, D. G. Mandrus, R. Arita, N. Trivedi, and J.-Q. Yan, Phys. Rev. B **92**, 100404(R) (2015).

[4] D. J. Singh, Phys. Rev. B **91**, 214420 (2015).

[5] I. I. Mazin and D. J. Singh, Phys. Rev. B **56**, 2556 (1997).

[6] P. Manuel, D. T. Adroja, P.-A. Lindgard, A. D. Hillier, P. D. Battle, W.-J. Son, and M.-H. Whangbo, Phys. Rev. B **84**, 174430 (2011).

[7] One may think of possible cancellation of errors, as for instance in FeTe, where the local moment is underestimated because of strong correlations, yet suppression of the ordered moment is also underestimated because of strong spin fluctuation. However, extremely high T_N indicates that fluctuations at low temperatures are weak, and cannot appreciably suppress the ordered moment. Indeed, calculations reported in Ref. [2], using a hybrid method enhancing on-site correlations, overestimate the equilibrium moment by nearly 50% (R. Walton, private communication).

[8] These authors report Monte Carlo simulations for the calculated set of parameters, and claim a good agreement with the experiment; however, their nearest-neighbor only simulations yielded an unphysical result of $T_N = JM^2$, which is the mean field temperature, rather than $T_N = 0$, as required by the Mermin-Wagner theorem, indicating that thermal fluctuations have not been properly accounted for in these simulations.

[9] K. Foyevtsova, H. O. Jeschke, I. I. Mazin, D. I. Khomskii, and R. Valenti, Phys. Rev. B **88**, 035107 (2013).

[10] R. D. Johnson, S. Williams, A. A. Haghighirad, J. Singleton, V. Zapf, P. Manuel, I. I. Mazin, Y. Li, H. O. Jeschke, R. Valenti, and R. Coldea, arXiv:1509.02670.

[11] D. Wang, W.-S. Wang, and Q.-H. Wang, Phys. Rev. B **92**, 075112 (2015).

[12] S. A. J. Kimber, I. I. Mazin, J. Shen, H. O. Jeschke, S. V. Streltsov, D. N. Argyriou, R. Valenti, and D. I. Khomskii, Phys. Rev. B **89**, 081408(R) (2014).

[13] P. Blaha, K. Schwarz, G. K. H. Madsen, D. Kvasnicka, and J. Luitz, WIEN2k, An Augmented Plane Wave + Local Orbitals Program for Calculating Crystal Properties (Techn. Universitat Wien, Wien, 2001).

[14] See Supplemental Material at http://link.aps.org/supplemental/10.1103/PhysRevB.92.134408 for computational details.

[15] G. Kresse and J. Furthmüller, Phys. Rev. B **54**, 11169 (1996).

[16] T. Moriya, *Spin Fluctuations in Itinerant Electron Magnetism* (Springer, Berlin, 2012).

[17] B. V. Costa and A. S. T. Pires, J. Magn. Magn. Mater. **262**, 316 (2003).

[18] C. Yasuda, S. Todo, K. Hukushima, F. Alet, M. Keller, M. Troyer, and H. Takayama, Phys. Rev. Lett. **94**, 217201 (2005).

[19] J. Mravlje, M. Aichhorn, and A. Georges, Phys. Rev. Lett. **108**, 197202 (2012).

[20] A. I. Poteryaev *et al.*, http://amulet-code.org.

[21] G. Biroli and G. Kotliar, Phys. Rev. B **65**, 155112 (2002).

[22] P. Werner, A. Comanac, L. de'Medici, M. Troyer, and A. J. Millis, Phys. Rev. Lett. **97**, 076405 (2006).

Supplemental materials: Localized itinerant electrons and unique magnetic properties of $SrRu_2O_6$. Calculation details.

S. V. Streltsov,[1,2] I. I. Mazin,[3] and K. Foyevtseva[4]

[1] *M.N. Miheev Institute of Metal Physics of Ural Branch of Russian Academy of Sciences, 620137, Ekaterinburg, Russia*
[2] *Ural Federal University, Mira St. 19, 620002 Ekaterinburg, Russia*
[3] *Code 6393, Naval Research Laboratory, Washington, DC 20375, USA*
[4] *Quantum Matter Institute, University of British Columbia, Vancouver, British Columbia V6T 1Z4, Canada*

(Dated: August 10, 2015)

The experimental crystal structure as reported in Ref. [1] has been used in all claculations.

VASP CALCULATIONS

The fixed-spin-moment calculations, presented in Fig. 3 of the main text and the simulations of magnetic energy and magnetic moment dependence on the canting angle of the spins were performed in the Vienna *Ab initio* Simulation Package (VASP)[2]. The total energy was calculated for 98 different combinations of the canting angle and magnitudes of the magnetic moments on Ru (Fig. S1), and subsequently fitted to the Hamiltonian described in the text. A contour plot of this total energy fit is shown in Fig. S2.

We used a mesh of 256 k-points in the VASP calculations. The plane-wave cut-off energy was chosen to be 700 eV. The generalized gradient approximation (GGA) with exchange-correlation potential proposed by Perdew, Burke, and Ernzerhof (PBE)[4] was utilized. The constrain parameter Λ was increased until convergence of better than 0.02 meV was achieved, which required increasing Λ up to 120.

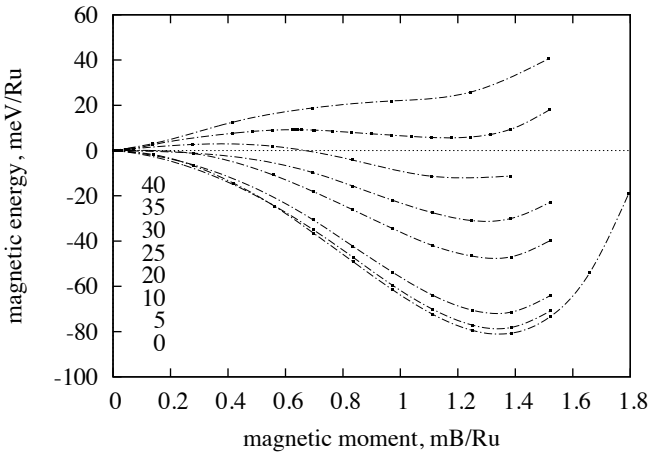

FIG. S1. Calculated energies for individual canting angles as a function of the magnetic moment. The lines are best fits of each set to the functional form $a_2M^2 + a_4M^4 + a_6M^6$.

LAPW CALCULATIONS

The electronic structure and total energies of different collinear magnetic configurations obtained in VASP were verified by full-potential linearized augmented plane-wave (LAPW) calculations, performed in the Wien2k package [3]. We also used the LAPW method for the projection of the Density of states (DOS) onto the corresponding molecular orbitals and for simulation of the magnetic moment and the doping dependence of total energies.

In LAPW calculations we also used the PBE version of the exchange correlation potential[4]. Integration was performed using the tetrahedron method on a mesh consisting of 400 k-points in the Brillouin-zone (BZ). The radii of atomic spheres were chosen to be 2.36, 1.93 and 1.72 a.u. for Sr, Ru, and O, respectively. The parameter of the plane wave expansion was set to $R_{MT}K_{max} = 7$, where R_{MT} is the radius of O and K_{max} is the plane wave cut-off.

In order to estimate the magneto-crystalline anisotropy

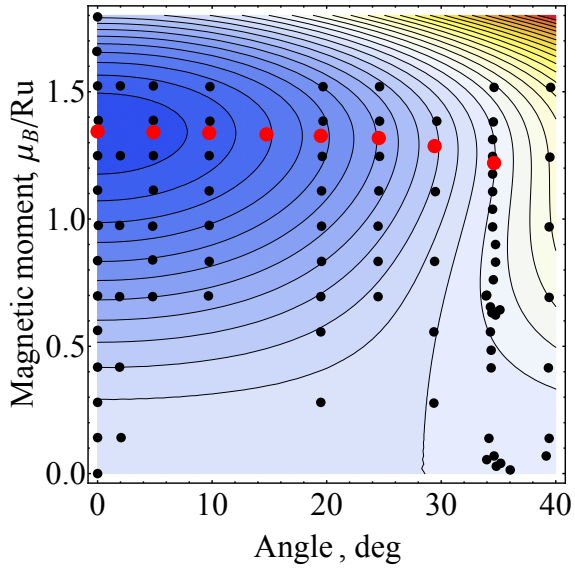

FIG. S2. Contour plot of the total energy fit described in the main text. The markers show locations of the first principle points. Red color indicates points obtained by fixing the angle and relaxing the magnitude of the moment.

we performed total energy calculations for several directions of the quantization axis taking into account the spin-orbit coupling. The number of $k-$points was increased up to 2000 in this case.

The doping dependence was simulated by changing the total number of carriers and screening it by an appropriate background charge. The crystal structure was not optimized in these calculations.

LDA+DMFT CALCULATIONS

We used the Quantum Espresso (QE) pseudopotential code [5] to generate the tight binding Hamiltonian used for the LDA+DMFT calculations. The choice of this calculation scheme was dictated by the available interface between QE and the Amulet code [6], which was used for the DMFT calculations. The GGA band structure obtained in the QE is close to the one calculated using the LAPW method, and the tight binding parameters are similar to those published by Tian *et al.*[8]

The Wannier projection technique [7] was applied to generate small 6×6 non-interacting Hamiltonian for the Ru t_{2g} states on a mesh of 3375 k-points. We use the interaction parameters $U = 2.7$ and $J = 0.3$ eV, as estimated in Ref. [8]. The calculations were performed for the Néel AFM structure. We used the continuous-time quantum Monte-Carlo (CT-QMC) solver [9].

[1] C. I. Hiley, M. R. Lees, J. M. Fisher, D. Thompsett, S. Agrestini, R. I. Smith, and R. I. Walton, Angew. Chem. Int. Ed. **53**, 4423 (2014)

[2] G. Kresse and J. Furthmaller, Phys. Rev. B **54**, 11169 (1996).

[3] P. Blaha, K. Schwarz, G. K. H. Madsen, D. Kvasnicka, and J. Luitz, WIEN2k, An Augmented Plane Wave + Local Orbitals Program for Calculating Crystal Properties (Techn. Universitat Wien, Wien, 2001).

[4] J. P. Perdew, K. Burke, and M. Ernzerhof, Phys. Rev. Lett. 77, 3865 (1996)

[5] P. Giannozzi et al, J. Phys. Condens. Matter **21**, 395502 (2009)

[6] http://www.amulet-code.org

[7] D. Korotin, A. V. Kozhevnikov, S. L. Skornyakov, I. Leonov, N. Binggeli, V. I. Anisimov, and G. Trimarchi, Eur. Phys. J. B **65**, 91 (2008).

[8] W. Tian, C. Svoboda, M. Ochi, M. Matsuda, H. B. Cao, J. Cheng, B. C. Sales, D. G. Mandrus, R. Arita, N. Trivedi, and J. Yan arxiv:1504.03642

[9] P. Werner, A. Comanac, L. De Medici, M. Troyer, and A. J. Millis, Phys. Rev. Lett. **97**, 076405 (2006).